American Mineralogist, Volume 91, pages 680–684, 2006

Synthetic Ag-rich tourmaline: Structure and chemistry

David London,[1,*] Andreas Ertl,[2] John M. Hughes,[3] George B. Morgan VI,[1] Eric A. Fritz,[4] and Brian S. Harms[1]

[1]School of Geology and Geophysics, University of Oklahoma, 100 East Boyd Street, Room 810 SEC, Norman, Oklahoma 73019, U.S.A.
[2]Institut für Mineralogie und Kristallographie, Geozentrum, Universität Wien, Althanstrasse 14, 1090 Vienna, Austria
[3]Department of Geology, Miami University, Oxford, Ohio 45056, U.S.A.
[4]Gemological Institute of America, 5345 Armada Drive, Carlsbad, California 92008, U.S.A.

Abstract

Ag-rich tourmaline crystals were synthesized at 750 °C, 200 MPa H_2O, and f_{O_2} = log (NNO) – 0.5, starting with an oxide mix of dravite composition to which various reagents, including AgF and AgCl, were added. Tourmaline containing up to 7.65 wt% Ag_2O was synthesized, and this is the first time a tourmaline is described that contains significant amounts of Ag at the ninefold-coordinated X site. Crystal structure refinement and chemical analysis (EMPA) give the optimized formula $^{X}(Na_{0.58}Ag_{0.18}\square_{0.24})$ $^{Y}(Al_{1.54}Mg_{1.46})$ $^{Z}(Al_{5.34}Mg_{0.66})$ $^{T}(Si_{5.90}Al_{0.10})O_{18}$ $(BO_3)_3$ $^{V}(OH)_3$ $^{W}(O_{0.53}F_{0.47})$, with a = 15.8995(4) and c = 7.1577(4) Å, and R = 0.036 for a crystal (~20 × 100 μm) with approximately 2.2 wt% Ag_2O. Refining Na ↔ Ag at the X site clearly indicates that Ag occupies this site. The X-O2 distance of ~2.52 Å is slightly longer than tourmaline with ~$(Na_{0.6}\square_{0.4})$, reflecting the slightly larger ionic radius of Ag compared to Na. Releasing the occupancy at the Y site gives ~$Al_{0.98}$ (~12.7 e^-), which can be explained by occupation of Mg and Al. On a bond-angle distortion vs. <Y-O> distance diagram, the Ag-rich olenite-dravite lies approximately on the V site = 3 (OH) line in the figure, defining the relation between bond-angle distortion (σ_{oct}^2) of the ZO_6 octahedron and the <Y-O> distance. No H could be found at the O1 site by refinement, in agreement with the Mg-Al disorder between the Y site and the Z site. Synthetic tourmaline contains no Ag when only AgCl is added; the compatibility of Ag in tourmaline, therefore, is largely a function of the F/Cl ratio of the fluid medium. A positive association of Ag at the X site with Al at the Y site and with F suggests that tourmaline might be useful for exploration in Cornwall-type polymetallic ore deposits associated with F-rich peraluminous granites or at other Ag-, F-, and B-enriched deposits such as Broken Hill, Australia. Preliminary electron microprobe analyses of tourmaline from Cornwall and Broken Hill, however, failed to detect Ag at the 3σ detection level of 0.08 wt% Ag_2O.

Keywords: Tourmaline, silver, crystal synthesis, crystal structure

Introduction

In natural tourmaline, $XY_3Z_6(BO_3)_3T_6O_{18}V_3W$ (Hawthorne and Henry 1999), the X site can be occupied by Na, Ca, K, or □, but Na predominates in the common solid-solutions among schorl-dravite-olenite-foitite. In the schorl-dravite series, $^{[9]}Na^+$ (ionic radius ~1.40 Å) occupies the X site, which has a polyhedral volume of 32–33 Å^3. Although schorl-dravite commonly crystallizes with K-feldspar, K normally is incompatible in tourmaline. Potassium contents rarely exceed 0.1 wt% K_2O in tourmaline, and the maximum recorded value is ~2.3 wt% K_2O in povondraite (Grice et al. 1993). Presumably, $^{[9]}K^+$ (ionic radius ~1.63 Å) is too large for the X site of tourmaline from the schorl-dravite-olenite-foitite series. The ionic radius of $^{[8]}Ag^+$ (~1.38 Å, no known data for $^{[9]}Ag^+$ or $^{[10]}Ag^+$) is 10% larger than $^{[8]}Na^+$(~1.24 Å) but 15% smaller than $^{[8]}K^+$ (~1.63 Å). Substitution of Ag^+ for Na^+, therefore, would produce a relatively small volume change of the XO_9 polyhedron. We confirm here that tourmaline can accommodate a significant fraction of the larger Ag^+ at the X site. We examine the chemistry and atomic arrangement of a synthetic tourmaline with a significant amount of Ag at the X site, and comment on the possible use of tourmaline as an indicator mineral in precious metal exploration.

Experimental details

Tourmaline synthesis

Different Ag-rich tourmaline samples were synthesized at 500–750 °C and 200 MPa H_2O in subhorizontal cold-seal pressure vessels, starting with an oxide mix, "Syntur," of the composition of dravite (Table 1), to which various reagents (including AgF and AgCl) were added. Deionized ultrafiltered water, then Ag halide, then Syntur mix were added to Au capsules 2.5 mm in diameter and 4–6 mm long. Capsules were sealed by DC argon-plasma arc-welding while keeping the capsule frozen to prevent volatilization of added water, placed overnight in an oven at 130 °C, and then re-weighed to ensure no leakage. Experiments were conducted in subhorizontal NIMONIC 105 cold-seal pressure vessels with water as the pressure medium. Variations in the target temperature and pressure during the experiments were ±3 °C and ±1 MPa, respectively. The temperature was monitored with an internal Chromel-Alumel thermocouple, and pressure was monitored with a factory-calibrated Heise bourdon tube gauge; uncertainties in temperature and

* E-mail: dlondon@ou.edu

pressure are <10 °C and <10 MPa, respectively. The experiments were quenched isobarically at ~75 °C/minute using a jet of air and water. After quench, capsules were weighed, punctured to check for free water, then opened. The f_{O_2} during experiments was log (NNO) – 0.5 based on our measurement of the solubility of cassiterite in hydrous granitic melt in relation to f_{O_2} (Linnen et al. 1996).

Preliminary experiments by Fritz (2001) produced tourmalines that contain up to 5.97 wt% Ag_2O (SD = 0.82), with a maximum single-point value of 7.65 wt% Ag_2O in experiment MnT62 (at 600 °C, 200 MPa H_2O). The latter experiment, however, utilized $MnBr_2$, $LiAlSiO_4$ (α-eucryptite), and AgF in addition to the Syntur mix. In general, the Ag content of tourmaline in the MnT-series experiments appeared to increase as the elbaite component increased (i.e., Li at the Y cite, as deduced from EMPA: Fig. 1). To more clearly assess the compatibility of Ag in a chemically simpler system, the subsequent experiments ST-62, ST-63, and ST-70 were performed using only the Syntur mix, AgF or AgCl, and added water. Fluorine was added as AgF, which decomposed during the experiments to release F (and formed MgF_2 and cryolite precipitates in some experiments). Although Ag normally alloys with the Au of the capsule tube when AgF decomposes, energy-dispersive X-ray analysis indicated that Ag was incorporated into the tourmaline crystals (as observed for synthetic Mn-rich dravite crystals by Ertl et al. 2003b). Tourmaline with high Ag content coexisted with Ag oxide, Mg fluoride, cryolite, and a presently unidentified Na-Ni micaceous phase (in H_2O-pressurized cold-seal vessels, Ni diffuses from the reaction vessel through the Au tubing and into the contents of the reaction assemblage). The Ag-rich tourmaline described in this work was synthesized at 750 °C and 200 MPa H_2O, starting with Syntur + AgF + H_2O. A colorless single tourmaline crystal (~20 μm in diameter, ~100 μm in length), similar to the large crystal in the center of Figure 2, was selected from the synthetic product ST-70 for crystal-structure refinement. A similar experiment containing AgCl instead of AgF also produced tourmaline. Attempts to synthesize end-member Ag-Mg tourmaline (Na-absent) failed to produce tourmaline under similar experimental conditions.

Crystal structure of Ag-bearing tourmaline

The tourmaline crystal was mounted on a Bruker Apex CCD diffractometer equipped with graphite-monochromated Mo*K*α radiation. Redundant data were collected for an approximate sphere of reciprocal space, and were integrated and corrected for Lorentz and polarization factors using the Bruker program SAINT-PLUS (Bruker AXS Inc. 2001). The refined cell-parameters and other crystal data are listed in Table 2.

The structure was refined using the tourmaline starting model and the Bruker SHELXTL v. 6.10 package of programs, with neutral-atom scattering factors and terms for anomalous dispersion. Refinement was performed with anisotropic-displacement parameters for all non-hydrogen atoms. Table 3 lists atom parameters and Table 4 lists selected interatomic distances.

TABLE 1. Weight fractions of oxide components in SYNTUR mix

Component	Wt%
SiO_2	35.49
Al_2O_3	30.14
MgO	12.34
$Na_2B_4O_7 \cdot 10H_2O$	10.73
B_2O_3	11.29
Sum	99.99

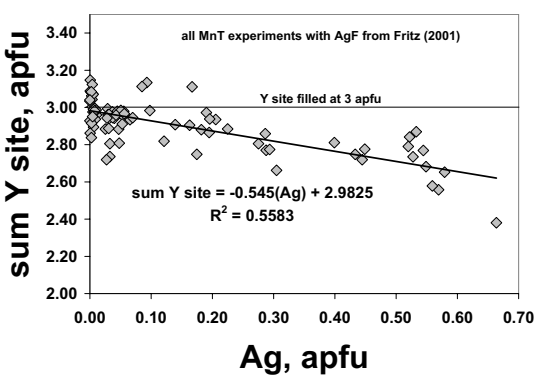

FIGURE 1. Graph of Ag vs. total occupancy of the Y site (Fe^{2+} + Mg^{2+} + Al^{3+}) of synthetic tourmaline based on EMPA, from Fritz (2001).

Chemical analysis

All elements (except B and H) were determined by electron microprobe analysis (EMPA) at the University of Oklahoma using a Cameca SX50 equipped with five wavelength-dispersive spectrometers. Operating conditions were 20 kV accelerating voltage, 15 nA beam current, and 2 μm spot size. Peaks for all elements were measured for 15 s, except for F (45 s). Natural and synthetic crystalline materials were used as standards, and data reduction used the PAP procedure (Pouchou and

TABLE 2. Crystal data and results of structure refinement for synthetic Ag-rich tourmaline

Unit cell by least squares	a = 15.8995(4) Å
(space group: *R*3*m*, 5570 reflections):	c = 7.1577(4) Å
Frame width, scan time, number of frames:	0.20°, 15 s, 4500
Detector distance:	5 cm
Effective transmission:	0.794–1.000
R_{int} (before - after SADABS absorption correction):	0.0594–0.0463
Measured reflections, full sphere:	10,825
Unique reflections - refined parameters:	1113–94
*R*1 (%):	3.7 for 1100 $F_o > 4\sigma(F_o)$ and 3.7 for all 1113 data
Largest difference peaks:	+0.73, –0.82 e^-·Å^{-3}
Goodness-of-Fit:	1.14

TABLE 3. Atomic positions equivalent-isotropic U for atoms in synthetic Ag-rich tourmaline

Atom	*x*	*y*	*z*	U_{eq}	Occ.
Na	0	0	3/4	0.0186(9)	$Na_{0.891(5)}$
Ag	0	0	3/4	0.0186(9)	$Ag_{0.109}$
Si	0.80832(6)	0.81032(6)	0.9752(4)	0.00571(19)	$Si_{1.00}$
B	0.8903(2)	0.7807(4)	0.5220(8)	0.0083(9)	$B_{1.00}$
AlY	0.87520(11)	0.93760(6)	0.3440(4)	0.0109(5)	$Al_{0.980(9)}$
AlZ	0.70238(7)	0.73859(7)	0.3647(4)	0.0063(2)	$Al_{1.00}$
O1	0.0000	0.0000	0.2057(8)	0.0114(11)	$O_{1.00}$
O2	0.93904(13)	0.8781(3)	0.4877(6)	0.0123(7)	$O_{1.00}$
O3	0.7365(3)	0.86825(15)	0.4655(6)	0.0115(7)	$O_{1.00}$
O4	0.90628(14)	0.8126(3)	0.9039(6)	0.0115(7)	$O_{1.00}$
O5	0.8145(3)	0.90727(13)	0.8815(6)	0.0112(6)	$O_{1.00}$
O6	0.80489(17)	0.81525(17)	0.2000(5)	0.0092(4)	$O_{1.00}$
O7	0.71404(17)	0.71441(16)	0.8975(5)	0.0086(4)	$O_{1.00}$
O8	0.78999(17)	0.72960(18)	0.5356(5)	0.0098(5)	$O_{1.00}$
H3	0.743(5)	0.871(2)	0.563(10)	0.008(15)	$H_{1.00}$

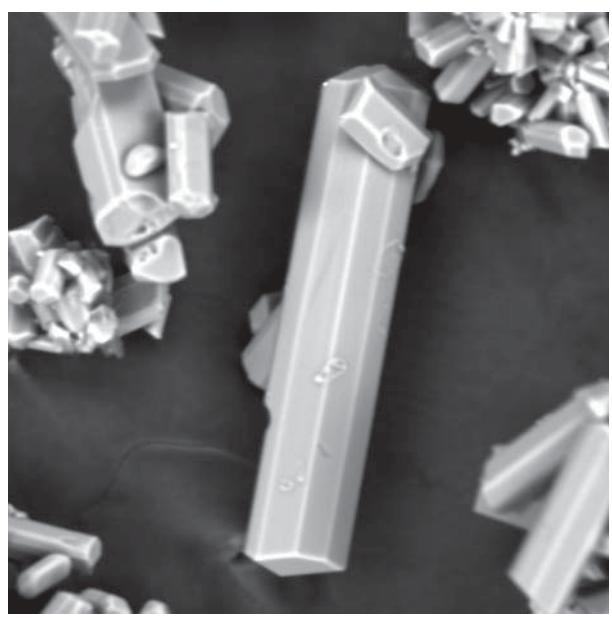

FIGURE 2. Backscattered electron image of synthetic Ag-rich tourmaline (ST-70) with a very coarse grained Ag-rich tourmaline crystal ~30 × 140 μm. Image size 158 × 158 μm.

TABLE 4. Selected interatomic distances in synthetic Ag-rich tourmaline

X-	O2 (×3)	2.519(4)	Y-	O6 (×2)	1.980(3)
	O5 (×3)	2.722(4)		O1	1.983(3)
	O4 (×3)	2.806(4)		O2 (×2)	1.983(3)
Mean	2.682		O3	2.099(4)	
		Mean	2.001		
Z-	O6	1.883(3)	T-	O7	1.611(2)
	O8	1.886(3)		O6	1.614(3)
	O7	1.896(2)		O4	1.622(1)
	O8′	1.912(3)		O5	1.638(2)
	O7′	1.941(2)	Mean	1.621	
	O3	1.987(2)			
Mean	1.918	B-	O2	1.364(6)	
			O8 (×2)	1.385(4)	
		Mean	1.378		

Pichoir 1985). Under the described conditions, analytical errors for all analyses are ± 1% relative for major elements and ± 5% relative for minor elements. With the methods used, the 3σ detection level for Ag was 0.08 wt% Ag_2O.

RESULTS AND DISCUSSION

Crystal chemistry

Analyses of experiments by Fritz (2001) provided early indications that Ag could occupy a structural site in synthetic tourmaline, which lacked resolvable Ag metal or oxide blebs. Additional confirmation comes from a comparison of experiments ST-62 with AgF and ST-63 with AgCl. The experiment with AgCl contains no measurable Ag in the tourmaline (Table 5); if the Ag were simply particulate metal or oxide, tourmaline in both experiments should be contaminated similarly. Silver and Na in tourmaline vary inversely (Fig. 3a), which is consistent with Ag at the X site. Note that the highest Ag content was recorded in the short duration AgF experiment (ST-62) and in the cores of larger crystals grown over a longer time period (ST-70), but that the Ag content of tourmaline falls off toward the rims of large crystals in ST-70 and in the finer-grained tourmaline from the same experiment. This trend reflects loss of Ag to the Au capsule with time, and recrystallization (Ostwald ripening) of tourmaline grains as reported by Palmer et al. (1992). There is no significant variation of Ag with Al at the Y site (Fig. 3b); all of the synthetic tourmaline contains appreciable Al at Y. Analyses of tourmaline in experiment ST-62, however, do show a positive correlation of Ag with Al at Y, which corresponds to the operation of an exchange component, $(Ag^XAl^YO^W)[Na^XMg^Y(OH)^W]_{-1}$, relative to end-member dravite. The tourmaline richest in Ag is also most enriched in F, though Figure 3c shows that the F content of tourmaline remains constant in ST-70 despite a progressive drop in Ag. It is possible to explain the compositional variations in ST-70 as a result of $NaAg_{-1}$ exchange during Ostwald ripening of the initial tourmaline crystals, and to attribute the constancy of F to the buffering effect of associated fluorides during recrystallization of tourmaline. Despite the lack of clear trends relating Ag to F content, Ag clearly is compatible in tourmaline when F is present in the system, but is highly incompatible when F is absent.

Crystal structure

Using quadratic programming methods, Wright et al. (2000) offered a method of optimizing the occupants of cation sites in minerals with multiply occupied cation sites. The optimized formula minimizes the differences between the formula obtained

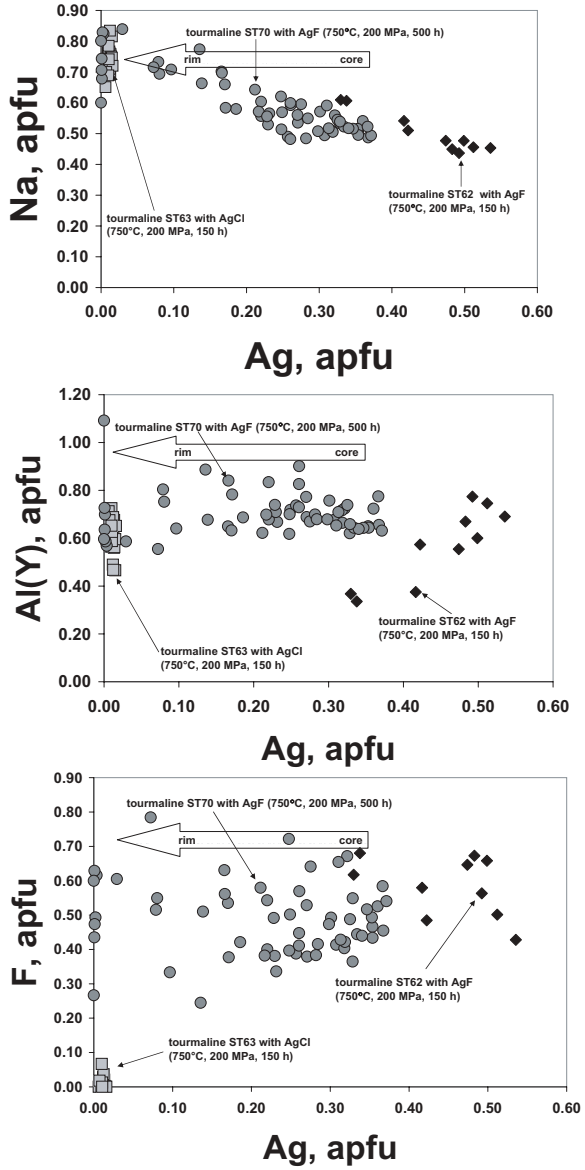

FIGURE 3. Comparison of tourmaline composition in experiments with AgF (ST-62, ST-70) and with AgCl (ST-63). Cation plots from EMPA of (**a**) Na vs. Ag, (**b**) Ag vs. Al in the Y site of tourmaline as calculated from the EMPA, and (**c**) Ag vs. F.

from the results of the chemical analysis and that obtained by single-crystal structure refinement (SREF). The structure refinement and chemical data obtained in this study by that method yields a structural formula for this synthetic Ag-bearing tourmaline of:

$$^X(Na_{0.58}Ag_{0.18}\square_{0.24})\,^Y(Al_{1.54}Mg_{1.46})\,^Z(Al_{5.34}Mg_{0.66})\,^T(Si_{5.90}Al_{0.10})O_{18}(BO_3)_3\,^V(OH)_3\,^W(O_{0.53}F_{0.47})$$

In reference to tourmaline end-member species (Hawthorne and Henry 1999), we can describe this tourmaline as a mixture of olenite (51 mol%) and dravite (49 mol%). Hence, this tourmaline belongs to the olenite-dravite series as do the tourmaline samples

TABLE 5. Average compositions of synthetic tourmaline from EMPA

	ST-70, core $n = 7$	ST-70, rim $n = 9$	ST-62 $n = 10$	ST-63 $n = 21$
Component				
SiO_2	36.43 (0.70)	37.40 (1.25)	33.80 (1.04)	33.96 (1.04)
Al_2O_3	36.67 (0.54)	37.13 (1.09)	35.29 (1.18)	37.73 (1.18)
FeO	0.02 (0.01)	0.07 (0.02)	0.02 (0.01)	0.01 (0.01)
MnO	0.01 (0.01)	0.01 (0.01)	0.01 (0.01)	0.01 (0.01)
MgO	9.23 (0.23)	9.84 (1.27)	9.46 (0.31)	10.32 (0.31)
NiO	0.02 (0.02)	0.47 (0.66)	–	–
CaO	0.01 (0.01)	0.02 (0.01)	0.02 (0.01)	0.01 (0.01)
Ag_2O	3.07 (0.77)	0.53 (0.96)	5.20 (0.03)	0.14 (0.03)
Na_2O	1.86 (0.20)	2.51 (0.26)	1.55 (0.14)	2.37 (0.14)
F	0.90 (0.24)	1.45 (0.90)	1.11 (0.03)	0.02 (0.03)
Cl	0.01 (0.01)	0.01 (0.01)	0.01 (0.04)	0.10 (0.04)
O=F	–0.38 (0.10)	–0.61 (0.38)	–0.47 (0.01)	–0.01 (0.01)
O=Cl	–0.00 (0.00)	–0.00 (0.00)	–0.00 (0.01)	–0.02 (0.01)
Total	87.85 (0.38)	88.83 (0.45)	86.00 (0.61)	84.64 (0.61)
Formulae*				
T Site				
Si	5.739	5.711	5.567	5.456
Al	0.261	0.289	0.433	0.544
Z Site				
Al	6.000	6.000	6.000	6.000
Y Site				
Al	0.548	0.394	0.418	0.601
Fe	0.003	0.009	0.003	0.001
Mn	0.001	0.001	0.001	0.001
Mg	2.167	2.239	2.322	2.471
Ni	0.003	0.058	–	–
Y Sum	2.749	2.643	2.744	3.083
X Site				
Ca	0.002	0.003	0.004	0.002
Ag	0.251	0.042	0.444	0.012
Na	0.568	0.743	0.495	0.738
X Sum	0.821	0.788	0.943	0.752
O3 Site				
F	0.448	0.700	0.578	0.010
Cl	0.003	0.003	0.003	0.027

Notes: Numbers in parentheses indicate 1σ standard deviations.
* 24.5 total negative charge, excludes charge associated with an inferred stoichiometry of 1.5 B_2O_3 per formula unit.

described by Ertl et al. (2003a).

Refining Na ↔ Ag at the X site clearly indicates that Ag occupies this site (Table 3). An electron density of ~15 e^- at the X site can be explained by occupancies of ~($Na_{0.6}Ca_{0.4}$) or ~($Na_{0.6}Ag_{0.2}\square_{0.2}$). Because of the very low CaO content (0.01 wt%, Table 5), the X site can only be occupied by ~($Na_{0.6}Ag_{0.2}\square_{0.2}$). Ertl et al. (2001) showed that there is a reliable relation between the X-O2 distance and the occupancy of the X site. The X-O2 distance of ~2.52 Å for the Ag-bearing tourmaline is slightly longer than the ~2.4–2.50 Å distance observed for tourmaline with an X-site occupancy of ($Na_{0.6}\square_{0.4}$) (Bloodaxe et al. 1999), reflecting the slightly larger ionic radius of Ag compared to Na.

Releasing the occupancy at the Y site gives ~$Al_{0.98}$ (~12.7 e^-), indicating occupancy by Al and Mg in accord with the <Y-O> distance of 2.001 Å. Substitution of Al for Mg at the Z site has been described by Grice and Ercit (1993), Hawthorne et al. (1993), MacDonald and Hawthorne (1995), Taylor et al. (1995), Bloodaxe et al. (1999), and Ertl et al. (2003a). Significant amounts of Mg at the Z site are reflected in the <Z-O> distance. Tourmaline samples with similar lattice parameters but without Mg, where the Z site is only occupied by Al, show a <Z-O> distance of 1.908–1.910 Å (Ertl et al. 2003b, 2004; Nuber and Schmetzer 1981). The <Z-O> distance in the synthetic Ag-bearing tourmaline is 1.918 Å, which corresponds to some Mg at the Z site. The optimized formula yields 0.66 apfu Mg at the Z site, in good agreement with Bloodaxe et al. (1999), who observed 0.70 apfu Mg and $Al_{5.30}$ for their sample SmFalls, a schorl-dravite solid solution with the same <Z-O> distance as the synthetic Ag-bearing tourmaline.

The <T-O> distance of 1.621 Å (Table 4) is slightly enlarged relative to a site fully occupied with Si (1.620 Å; Hawthorne 1996; MacDonald and Hawthorne 1995; Bloodaxe et al. 1999; Ertl et al. 2001). Substitution of Al^{3+} for Si^{4+} was first proposed by Buerger et al. (1962). The relation between <T-O> distances and Al occupancy in the ring was first described by Foit and Rosenberg (1979) and Foit (1989). MacDonald and Hawthorne (1995) have shown by crystal-structure analysis in combination with chemical analysis that Mg-rich tourmaline samples can contain significant amounts of $^{[4]}Al$ (up to ~0.5 apfu). The optimized formula for the present Ag-rich tourmaline shows that the T site is occupied by ($Si_{5.90}Al_{0.10}$), in good agreement with the observed <T-O> distance (Formula 1 of Ertl et al. 2001). Because there is no indication of $^{[4]}B$, we set the B content at 3.00 apfu (Table 5).

A hydrogen atom at the site associated with O3 (= H3) was easily located in this refinement. Ertl et al. (2002) showed that the bond-angle distortion (σ_{oct}^2) of the ZO_6 octahedron in tourmaline is largely a function of the <Y-O> distance of that tourmaline, although occupancy at the O3 site (V site) also affects the distortion. The covariance, r, of <Y-O> and the σ_{oct}^2 of the ZO_6 octahedron is –0.991 (Fig. 4) for all investigated tourmalines that have 3 (OH) groups at the O3 site, including the samples from Hughes et al. (2004). In Figure 4, the present tourmaline lies approximately on the V site = 3 (OH) line, with a slight tendency toward buergerite, which contains 0.3 (OH) and 2.7 O at the V site (Dyar et al. 1998). Hence, the V site is occupied almost completely by 3 (OH). No H was found at the W site (O1 site). Furthermore, it is not likely that the W site contains significant OH because of the relatively high total sum of the EMPA (Table 5) and because of the previously mentioned slight tendency of the V-site occupation toward the (OH-poor) buergerite. Normally, the V site must be completely filled by OH before significant OH can occur at the W site (e.g., Ertl et al. 2005). The dominance of O^{2-} at the W site can be explained by Mg-Al disorder between the Y site and the Z site (Taylor et al. 1995). This disorder is driven by the short-range requirements of O^{2-} at the O1 site that is associated with 2Al + Mg configurations at the coordinating Y sites so as to satisfy the bond-valence requirements of O^{2-} at the O1 site (Hawthorne 1996, 2002).

Applications

This study is relevant to the stability of tourmaline, and to the size and range of cations that it can accommodate at the X site. The positive association of Ag with Al at the Y site and with F, however, suggests that tourmaline might be useful for precious-metal exploration in Cornwall-type polymetallic ore deposits associated with F-rich peraluminous granites, or other Ag- and F-enriched deposits such as Broken Hill, New South Wales, Australia. An EMPA survey of tourmaline from various Cornish granites and wallrock-hosted tourmaline-cassiterite lodes (from the sample set studied by London and Manning 1995), none with known Ag mineralization, failed to detect Ag above background. Similarly, Ag was below detection in

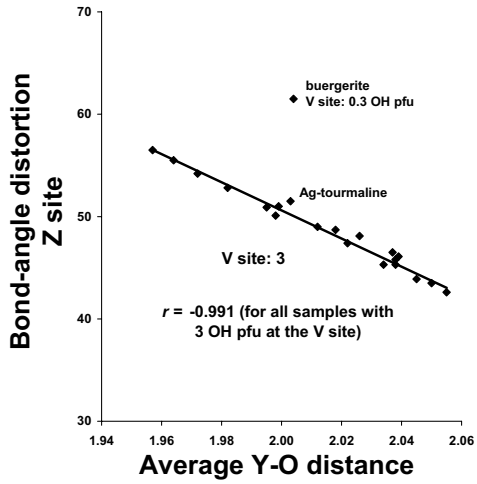

FIGURE 4. Relationship between bond-angle distortion (σ_{oct}^2) of the ZO_6 octahedron and the average Y-O distance. Modified from Figure 3 of Ertl et al. (2002), including the structural data of Hughes et al. (2004).

one sample from Broken Hill (provided by John Slack, U.S. Geological Survey, Reston, Virginia). The Cornish granites have the necessary chemistry to produce an Ag-enriched tourmaline (e.g., London and Manning 1995), but the fluids from which the tourmaline grew likely were not close to saturation in Ag or Ag_2O. At Broken Hill, a high abundance of sulfide would reduce the activity of Ag_2O needed as a component of tourmaline. Patterns of Ag distributions within tourmaline may emerge with more sensitive analytical methods.

Though very fine-grained, the Ag-rich tourmaline appears colorless in plane-polarized white light. Appreciable Ag in a synthetic tourmaline (e.g., up to ~7 wt% Ag_2O as reported here) would increase the density, and hence refractive index, without contributing color directly. The resultant increase in refractive indices might make this a useful additive for more brilliant synthetic tourmaline gemstones.

ACKNOWLEDGMENTS

This work was supported in part by NSF grants EAR-0124179, EAR-990165, and EAR-9618867 to DL; and NSF grants EAR-9804768, and EAR-0003201 to J.M.H. We sincerely thank F.C. Hawthorne and C.M. Clark for their careful reviews of the manuscript.

REFERENCES CITED

Bloodaxe, E.S., Hughes, J.M., Dyar, M.D., Grew, E.S., and Guidotti, C.V. (1999) Linking structure and chemistry in the schorl-dravite series. American Mineralogist, 84, 922–928.

Buerger, M.J., Burnham, C.W., and Peacor, D.R. (1962) Assessment of the several structures proposed for tourmaline. Acta Crystallographica, 15, 583–590.

Dyar, M.D., Taylor, M.E., Lutz, T.M., Francis, C.A., Guidotti, C.V., and Wise, M. (1998) Inclusive chemical characterization of tourmaline: Mössbauer study of Fe valence and site occupancy. American Mineralogist, 83, 848–864.

Ertl, A., Hughes, J.M., and Marler, B. (2001) Empirical formulae for the calculation of <*T*-O> and *X*-O2 bond lengths in tourmaline and relations to tetrahedrally-coordinated boron. Neues Jahrbuch Mineralogie Monatshefte, 12, 548–557.

Ertl, A., Hughes, J.M., Pertlik, F., Foit, F.F., Jr., Wright, S.E., Brandstätter, F., and Marler, B. (2002) Polyhedron distortions in tourmaline. Canadian Mineralogist, 40, 153–162.

Ertl, A., Hughes, J.M., Brandstätter, F., Dyar, M.D., and Prasad, P.S.R. (2003a) Disordered Mg-bearing olenite from a granitic pegmatite at Goslarn, Austria: A chemical, structural, and infrared spectroscopic study. Canadian Mineralogist, 41, 1363–1370.

Ertl, A., Hughes, J.M., Prowatke, S., Rossman, G.R., London, D., and Fritz, E.A. (2003b) Mn-rich tourmaline from Austria: Structure, chemistry, optical spectra, and relations to synthetic solid solutions. American Mineralogist, 88, 1369–1376.

Ertl, A., Schuster, R., Prowatke, S., Brandstätter, F., Ludwig, T., Bernhardt, H.-J., Koller, F., and Hughes, J.M. (2004) Mn-rich tourmaline and fluorapatite in a Variscan pegmatite from Eibenstein an der Thaya, Bohemian massif, Lower Austria. European Journal of Mineralogy, 16, 551–560.

Ertl, A., Rossman, G.R., Hughes, J.M., Prowatke, S., and Ludwig, T. (2005) Mn-bearing "oxy-rossmanite" with tetrahedrally-coordinated Al and B from Austria: structure, chemistry, and infrared and optical spectroscopic study. American Mineralogist, 90, 481–487.

Foit, F.F., Jr. (1989) Crystal chemistry of alkali-deficient schorl and tourmaline structural relationships. American Mineralogist, 74, 422–431.

Foit, F.F., Jr. and Rosenberg, P.E. (1979) The structure of vanadium-bearing tourmaline and its implications regarding tourmaline solid solutions. American Mineralogist, 64, 788–798.

Fritz, E. (2001) The compatibility of manganese +II in tourmaline, 93 p. Unpublished M.Sc. Thesis, University of Oklahoma.

Grice, J.D. and Ercit, T.S. (1993) Ordering of Fe and Mg in the tourmaline crystal structure: The correct formula. Neues Jahrbuch Mineralogie Abhandlungen, 165, 245–266.

Grice, J.D., Ercit, T.S., and Hawthorne, F.C. (1993) Povondraite, a redefinition of the tourmaline ferridravite. American Mineralogist, 78, 433–436.

Hawthorne, F.C. (1996) Structural mechanisms for light-element variations in tourmaline. Canadian Mineralogist, 34, 123–132.

——— (2002) Bond-valence constraints on the chemical composition of tourmaline. Canadian Mineralogist, 40, 789–797.

Hawthorne, F.C. and Henry, D.J. (1999) Classification of the minerals of the tourmaline group. European Journal of Mineralogy, 11, 201–215.

Hawthorne, F.C., MacDonald, D.J., and Burns, P.C. (1993) Reassignment of cation site-occupancies in tourmaline: Al-Mg disorder in the crystal structure of dravite. American Mineralogist, 78, 265–270.

Hughes, J.M., Ertl, A., Dyar, M.D., Grew, E., Wiedenbeck, M., and Brandstätter, F. (2004) Structural and chemical response to varying $^{[4]}B$ content in zoned Fe-bearing olenite from Koralpe, Austria. American Mineralogist, 89, 447–454.

Linnen, R.L., Pichavant, M., and Holtz, F. (1996) The combined effects of f_{O_2} and melt composition on SnO_2 solubility and tin diffusivity in haplogranitic melts. Geochimica et Cosmochimica Acta, 60, 4965–4976.

London, D. and Manning, D.A.C. (1995) Compositional variation and significance of tourmaline from southwest England. Economic Geology, 90, 495–519.

MacDonald, D.J. and Hawthorne, F.C. (1995) The crystal chemistry of Si ↔ Al substitution in tourmaline. Canadian Mineralogist, 33, 849–858.

Nuber, B. and Schmetzer, K. (1981) Strukturverfeinerung von Liddicoatit. Neues Jahrbuch für Mineralogie Monatshefte, 1981, 301–304.

Palmer, M.R., London, D., Morgan, G.B., VI, and Babb, H.A. (1992) Experimental determination of fractionation of $^{11}B/^{10}B$ between tourmaline and aqueous vapor: A temperature- and pressure-dependent isotopic system. Chemical Geology (Isotope Geoscience Section), 101, 123–129.

Pouchou, J.L. and Pichoir, F. (1985) "PAP" φ(ρz) correction procedure for improved quantitative microanalysis, p. 104–106. In J.T. Armstrong, Ed., Microbeam Analysis. San Francisco Press, California.

Taylor, M.C., Cooper, M.A., and Hawthorne, F.C. (1995) Local charge-compensation in hydroxyl-deficient uvite. Canadian Mineralogist, 33, 1215–1221.

Wright, S.E., Foley, J.A., and Hughes, J.M. (2000) Optimization of site-occupancies in minerals using quadratic programming. American Mineralogist, 85, 524–531.

MANUSCRIPT RECEIVED APRIL 4, 2005
MANUSCRIPT ACCEPTED JULY 21, 2005
MANUSCRIPT HANDLED BY PETER BURNS